

CLASSIFICATION OF SATELLITE IMAGES USING DEEP LEARNING FOR DISASTER MANAGEMENT

Prabha S

Assistant Prof. Department of Information Technology
Panimalar Engineering College, Chennai
prabha.mamce@gmail.com

Abinaya M

Department of Information Technology
Panimalar Engineering College, Chennai
abinayamurugan206@gmail.com

Preethi N

Department of Information Technology
Panimalar Engineering College, Chennai.
nagarathinampreethi@gmail.com

Priyadharshini C

Department of Information Technology
Panimalar Engineering College, Chennai.
paulinec146@gmail.com

Abstract— Satellite imagery plays a crucial role across diverse domains, encompassing agriculture, urban planning, disaster management, and environmental monitoring. The precise and effective categorization of satellite images is vital for extracting valuable insights and facilitating well-informed decision-making. In this investigation, we suggest leveraging artificial intelligence methodologies for the classification of satellite images. We compile a comprehensive dataset of labelled satellite images, representing various land cover types or objects of interest. Prior to analysis, the dataset undergoes preprocessing to enhance image quality, eliminate noise, and standardize the data. To augment the dataset and enhance the model's ability to generalize, we employ techniques such as rotation, scaling, and flipping. Future research avenues could involve exploring advanced deep learning architectures, including attention mechanisms or graph neural networks, to further elevate classification performance. Moreover, the incorporation of multi-sensor satellite data and temporal

analysis holds promise for augmenting classification models, particularly in dynamic monitoring and change detection applications.

Keywords— Satellite images, image categorization, AI, CNNs, Deep learning, Augmented data, Land cover identification, Transfer learning.

INTRODUCTION

The primary objective of this project is to investigate and demonstrate the effectiveness of artificial intelligence (AI) techniques in the classification of satellite images. Specifically, we aim to develop and evaluate machine learning and deep learning models for accurately and efficiently classifying various land cover types and objects present within satellite imagery. It is focused on refining model architectures to effectively accommodate the distinctive characteristics of satellite imagery, including spatial intricacies, spectral variations, and

textural nuances. Also, we have included the dataset of satellite images containing disaster affected and unaffected areas. Our system classifies the image into six classes and also predicts whether the area present in the image is affected by the disaster or not. The scope of satellite image classification using deep learning techniques outlines a comprehensive exploration of how these advanced AI methods can revolutionize the accuracy, efficiency, and practical applicability of remote sensing data analysis for diverse real-world scenarios.

LITERATURE SURVEY

In the reference paper [1], the authors say that small scale satellite networks' routing techniques experiences various issues in routing overhead as well as forwarding efficiency due to the enlargement of satellite constellation. This research frames a vector forward path method for the working of large-scale multilayer satellites. This path is constructed on the location basis between the starting point and landing point. This path is used to forward the data packets which will be shielding the influence of satellite's movements during routing. This paper then suggest a dynamic route strategy for maintenance. In a multilayer satellite network, there are two duties to be done by the low orbit satellites which includes, calculating routing tables for a region and dynamically planning the routing paths. The middle layer satellites manage the vector path connections in multiple divisions. The forward mode framed on the basis of starting and landing point increases the forwarding efficiency and decreases the routing overhead. This shows us that vector segment routing has a drastic improvement in the performance including delay reduction, loss of packet rate, and increased throughput in a multi-layer satellite network. It also shows the efficiency of routing table update mechanism which helps in improving the overall network overhead and working of them.

In the reference paper [2], the authors explored that the Low earth Orbit (LEO) satellite networks has the greatest communication features having global attention and coverage. Due to the rise of user terminal requirements, the conventional storage methods like cloud computing doesn't help. Hence, we are moving towards the edge computing in and Orbital Edge Computing (OEC) to cope up with the high user demands and requirements. Hence the authors have proposed an algorithm using greedy strategy for LEO satellites called the OEC task allocation algorithm (OECTA). This

algorithm helps in providing high reliability and workspace for the base users as well. They have also conducted the evaluation assessment for the proposed algorithm. Evaluation results show that proposed algorithm works better for the LEO satellites reducing the delay and energy usage up to 20% efficiently.

In the reference paper [3], the authors find that the radio spectrum is occupied in large numbers due to the rise of satellite networks. This leads to requirement of finding higher frequencies to accommodate, but there are several problems caused by the surroundings and nature when higher frequencies are operated. Hence, its very crucial for the operators to operate with them. The authors' proposed system suggests a practical method for low orbit satellites using machine learning concepts. This channel suggests prediction analysis using deep learning and time series generator for loss. These approach helps in analysing the satellite motion and movements from various latitudes and longitudes. More over this approach proved that these deep learning models helps us in achieving real time measurements with various angles and elevations.

In the reference paper [4], the authors say that Internet of Things (IoT) is built by the engagement and connectivity provided by the satellite networks. Due to the heavy congestion in the density of IoT, satellite networks undergo various consequences in the performance metrics. This article proposes a solution to these problems by framing a balancing routing algorithm for LEO satellites. In this algorithm, we will feed the predictions of the IoT distribution nature as well as the LEO satellite nature which helps us to divide the satellite demand into predictable and unpredictable variations in terms of ranges. So, we will apply the global function strategy for the essential long fluctuations and local functions for the small fluctuations to see the desired output. By combining the local and global functions we can see an optimal allocation for the traffic with an increased performance as well. When examined with the existing single focussed approach this combination approach provides a great alternative for implementation in real time situation as well as the performance metrics are seemed to be improved as well along with communication bandwidth.

In the reference paper [5], the authors suggest that artificial intelligence helps in classifying the satellite images for the extraction of desired insights. Long ago, meteorologist used to eye inspect the acquired satellite images and noted own the inspected notes of them. Gradually computers came in existence and data have been acquired by those technologies. This paper proposes to use the image segmentation techniques for the examination of the input satellite images. The images will be divided into pixels and grouped to find the desired output. Earlier, the satellite images captured were of low resolution. Various techniques have been employed in improving the quality of the images. This system proposes the use of Convolution Neural Network to classify the images. In the reference paper [6], the authors addressed the localization between the ground to satellite images. Earlier, it was treated using the image retrieval from the original satellite images. It will be compared with the ground captured reference images and analysed for the results. This paper proposes a new ideology for more optimal visualization of the images. Here they have used the pixel identification methods to better match and compare the satellite images and the ground images. The main aim of this approach is to find the exact location and characteristics of a given

image cover. This approach has been great in terms of improving performance and efficiency of the identification process.

EXISTING SYSTEM

Combining low-resolution hyperspectral images (LR-HSI) with high-resolution multispectral images (HR-MSI) sourced from different satellites offers a promising strategy to enhance hyperspectral imagery (HSI) resolution. However, challenges arise from inconsistencies among imaging satellites, varying lighting conditions, and divergent imaging schedules, impeding LR-HSI and HR-MSI alignment with established observation models. Achieving alignment between LR-HSI and HR-MSI poses significant obstacles. To address these challenges, this study introduces novel observation models tailored for LR-HSIs and HR-MSIs from distinct satellites. Subsequently, a deep-learning-based framework is proposed to manage critical processes in multi-satellite HSI fusion, including image registration, blur kernel learning, and image fusion.

The framework initiates with the development of a convolutional neural network (CNN) dubbed RegNet, which computes pixel-wise offsets between LR-HSI and HR-MSI, aiding LR-HSI registration. Then, a concise network named BKLNet learns spectral and spatial blur kernels based on the newly defined observation models. BKLNet and RegNet undergo joint training. During the fusion stage, FusNet is trained using the spatial blur kernel to downsample registered data. Rigorous experiments demonstrate the framework's superior performance in achieving HSI registration accuracy and fusion precision.

This comprehensive approach addresses challenges associated with multi-satellite HSI fusion and underscores the efficacy of the proposed deep-learning-based framework through extensive experimentation, affirming its superiority in enhancing registration accuracy and fusion outcomes. However, the framework demands substantial computational resources, potentially restricting its practicality and accessibility for users with limited computing capabilities. Additionally, the described process is time-intensive and may not be efficient for real-time applications or scenarios necessitating prompt results.

PROPOSED SYSTEM

We introduced a system aimed at employing a deep learning algorithm for project development. In recent times, the significant impact of deep learning and artificial intelligence in diverse industries has prompted our initiative. Consequently, we endeavored to apply a deep learning algorithm to refine and advance our project, focusing on utilizing previously gathered data related to satellite images. Through the incorporation of satellite-derived images, we conducted the training of our model, necessitating preprocessing of the data to enhance prediction accuracy. Following the preprocessing phase, we proceeded to train the model and evaluated its performance using metrics. The accuracy score obtained served as a measure of the model's proficiency in learning from the provided input. We have constructed an application framework designed specifically for deployment purposes. Utilizing deep learning technology, we crafted a classification model, resulting in a more cost-effective development process. Although our

approach involves a higher time complexity, the overall development costs are significantly reduced.

Framework for Applications

Django is a Python web framework renowned for its ability to swiftly build secure and enduring websites at a high level. Developed by experienced programmers, Django simplifies many of the challenges inherent in web development, enabling you to focus on building your applications without having to begin from square one. Notably, Django is freely available and open source, supported by a dynamic and active community, comprehensive documentation, and a wide array of support options, both free and paid.

Construction of a Classification Model

From Fig. 1, we can deduce that Deep learning requires the gathering of large amounts of historical image data to adequately train and test the model, thereby ensuring precise predictions.

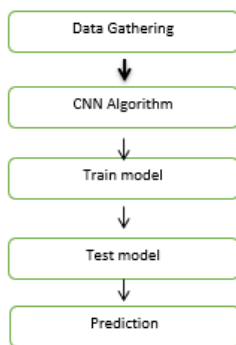


Fig. 1

Libraries Required

Tensorflow: Employed for utilizing TensorBoard, facilitating the comparison of loss and Adam curve in our result data or obtained logs.

Keras: Utilized for preprocessing the image dataset.

Matplotlib: Used to visualize and display the results of our predictive outcomes.

OS: Access to the files, enabling the reading of images from the train and test directories on our machines.

System Architecture

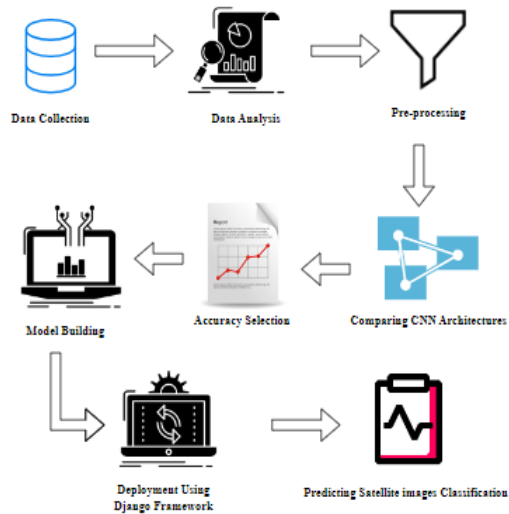


Fig. 2

MODULES

1. Data Analysis
2. Manual Architecture
3. Xception Architecture
4. Dense Net Architecture

1. Data Analysis

Data analysis encompasses the tasks of refining, modifying, and organizing raw data to derive meaningful, actionable insights beneficial for guiding business decisions. By engaging in this process, businesses mitigate decision-making risks through the acquisition of valuable insights. The process involved in this analysis include collecting comprehensive data sets, processing them, scrutinizing the data for patterns, and uncovering insightful observations. Specifically in the context of image data analysis, we examine the availability of data and assess the presence of regular data alongside masked data.

2. Manual Architecture

A Convolutional Neural Network (CNN), also known as ConvNet, is a specialized model within Deep Learning tailored for image analysis. It operates by assigning significance to various elements or objects in images using adjustable weights and biases, enabling effective differentiation between them. Unlike traditional classification algorithms, ConvNets require minimal preprocessing and can autonomously learn filters and features with adequate training data. Inspired by the connectivity pattern observed in the human brain's neurons, particularly the Visual Cortex, the architecture of ConvNets reflects this structure. Neurons in a ConvNet respond selectively to stimuli in specific visual field regions known as Receptive Fields.

3. Xception Architecture

Depthwise Separable Convolutions: Traditional convolutional methods typically apply multiple filters to input feature maps, leading to a heavy computational burden. In contrast, depthwise separable convolutions divide the conventional convolution process into two distinct stages: depthwise convolution and pointwise convolution.

Depthwise Convolution: During this stage, every channel within the input feature map undergoes convolution with its own set of filters autonomously. This implies that each channel is processed independently, without incorporating information from other channels.

Pointwise Convolution: During this phase, a 1×1 convolution is utilized to combine the results of the depthwise convolution, resulting in the final output feature map. Pointwise convolutions enable efficient integration and fusion of information from different channels. By employing depthwise separable convolutions, Xception achieves reduction in the number of coefficients compared to conventional convolutions, while maintaining a comparable level of accuracy.

Skip Connections: Xception incorporates skip connections, also referred to as shortcut connections, within its network architecture. These connections allow gradients to move directly between non-adjacent layers during training. By integrating skip connections, Xception mitigates the problem of vanishing gradients and simplifies the training of exceptionally deep networks.

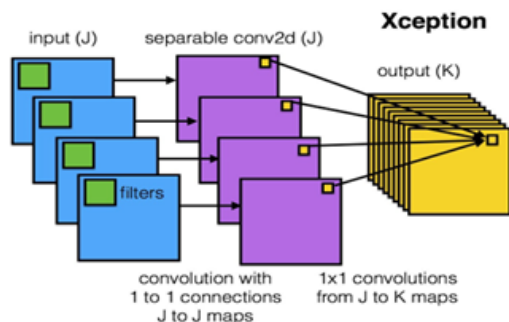


Fig. 3. Xception Architecture

4. Dense Net Architecture

Dense Connectivity: DenseNet introduces dense connections between its layers, establishing connections in which each layer is linked to all preceding and subsequent layers in a feed-forward manner. This dense connectivity fosters the construction of a deeply layered network, enhancing feature reuse and facilitating the smooth flow of information across the network.

Growth Rate: DenseNet manages the quantity of feature maps learned per layer using a parameter termed the growth rate. This rate dictates the number of new feature maps incorporated into each layer relative to the input feature maps. Serving as a bottleneck, it ensures the network remains compact and efficient in its operations.

Transition Layers: In DenseNet, transition layers play a crucial role in controlling spatial dimensions and reducing the number of feature maps before forwarding them into the next dense

block. These transition layers usually comprise a batch normalization layer, a 1x1 convolutional layer, and an average pooling layer. The average pooling layer decreases spatial dimensions, while the 1x1 convolutional layer diminishes the number of feature maps, effectively compressing the information.

Batch Normalization and ReLU: In DenseNet, batch normalization and ReLU activation functions are applied consecutively after each convolutional layer. Batch normalization stabilizes and accelerates training by standardizing the input to each layer, while ReLU introduces non-linearity, enhancing the network's ability to capture complex patterns within the data.

Dense Blocks: DenseNet consists of several dense blocks, each comprising numerous densely connected layers, as shown in Fig. 4. These dense blocks are connected by transition layers, as discussed earlier. The architecture can be configured in various ways depending on the depth and complexity required for a particular task.

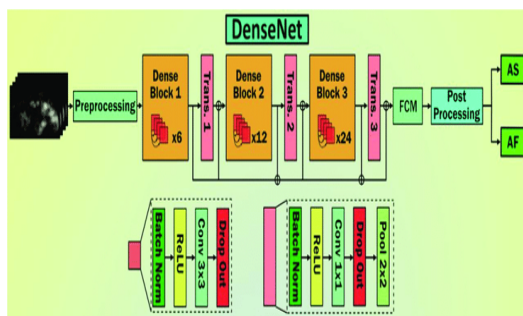


Fig. 4. Dense Net Architecture

Deploy

In this module, following the training of the deep learning model, it undergoes conversion into a format file (.h5 file). Post-conversion, the file is incorporated into our Django framework, enhancing the user interface and enabling output predictions. The system's functionality encompasses identifying whether the provided OCT image corresponds to CNV, DME, DRUSEN, or NORMAL conditions, thereby enriching the overall user experience with detailed insights.

CNN MODEL

Input layer

In a CNN, the Input Layer manages image data, which is presented as three-dimensional matrices. These matrices need to be reshaped into a single column before entering the network. For example, an image measuring 28 x 28 (784 pixels) is turned into a column of size 784 x 1 for processing.

The most essential parameters in a deep CNN are often found in the Input Layer, where user-defined settings, like the number and size of kernels, hold significant importance.

Convo layer

The convolutional layer, also referred to as the feature extractor layer, is tasked with extracting features from the image data. Initially, a portion of the image connects to the convolutional layer to undergo the process. This process involves computing the dot product between the receptive field (a local region of the input image matching the filter size) and the filter, resulting in a single value representing the output volume. Subsequently, the filter moves across the next receptive field of the same input image based on a specified stride and repeats the operation. This iterative process continues until the entire image is processed, generating the output used as input for the subsequent layer.

Pooling layers

Pooling layers serve a distinct function. Max pooling extracts the maximum value within a specified filter region, while average pooling computes the mean value within the same region. These operations are commonly used to decrease network dimensionality.

Fully connected layers

In this algorithm, the fully connected layers come before the classification output, flattening the results to prepare for classification. This arrangement closely resembles the output layer of a Multilayer Perceptron (MLP).

Softmax layer

The Softmax or Logistic layer functions as the ultimate layer in this CNN algorithm, typically situated at the conclusion of the Fully Connected layer. Logistic regression is applied for binary classification tasks, while softmax regression is utilized for multi-class classification objectives.

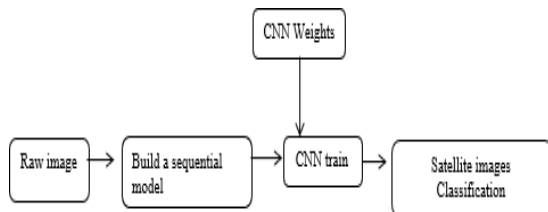
Output layer

The output layer embodies labels expressed through one-hot encoding. This encoding mechanism assigns a unique binary vector to each label, where only one element is designated as 1, while the remaining elements are set to 0.

METHODOLOGY

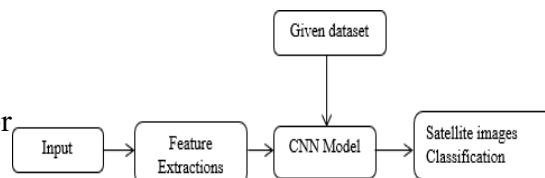
Preparing and training a Convolutional Neural Network (CNN) encompasses multiple phases. This process involves preprocessing the dataset, which includes activities like reshaping, resizing images, and converting them into an array format. The same preprocessing steps are applied to test images. The dataset comprises approximately four unique satellite images, and any of these images can be selected as a test image for the software. The method for identifying satellite images utilizes a two-channel structure capable of categorizing satellite images, as demonstrated in fig. 5.a and fig.b. In this approach, satellite images are inputted into the inception layer of the Convolutional Neural Network (CNN). Throughout the training process, the CNN conducts both feature extraction and classification tasks.

(a)



(b)

Fig. 5. a and b Two channel architecture for classification



DATASETS

This dataset consists of approximately train and test image records containing extracted features, which were subsequently classified into 5 classes: Cloudy, Desert, Wildfire, Water, and Green area.

Cloudy

This satellite image Fig. 6.a. captures a scene characterized by extensive cloud cover, with a dense layer of clouds spread across the entire frame. The clouds exhibit varying shades of white and gray, indicating different thicknesses and heights. The atmospheric conditions suggest a potentially overcast or rainy day, limiting the visibility of underlying features on the Earth's surface.

Desert

This high-resolution satellite image Fig. 6.b. captures a vast expanse of a desert landscape, characterized by its arid and barren features. The scene is dominated by a seemingly endless sea of golden sand dunes, sculpted by the wind into mesmerizing patterns and ripples. The absence of significant water bodies and the prevalence of dry, cracked terrain underscore the extreme nature of this desert ecosystem.

Wildfire

From fig.6.c. we infer a mosaic of fiery red and orange hues dominates the frame, representing active flames consuming vegetation across a significant expanse. Smoke billows upwards, forming thick plumes that blend with the atmosphere, obscuring the surrounding landscape. The presence of structures, roads, or natural barriers may indicate potential areas of impact or the direction of the fire's spread. This dataset serves as a critical tool for assessing the extent, intensity, and progression of wildfires, aiding in emergency response, resource allocation, and environmental impact analysis.

Water

Fig. 6.d. captures a serene and aqueous landscape, showcasing various water features with remarkable clarity. Large bodies of water, such as lakes, rivers, or oceans, stand out in deep blue and turquoise hues, reflecting the sunlight. Meandering rivers create sinuous patterns across the terrain, while coastal areas exhibit distinct shades where land meets the sea. The image also reveals intricate details such as currents, ripples, and waves, providing insights into the dynamic nature of the water bodies.

Green Area

In Fig. 6.e. a lush and vibrant green area, presenting a mosaic of dense vegetation and diverse flora. The landscape is dominated by a rich spectrum of green tones, indicative of thriving plant life. The verdant expanse includes dense forests, meadows, or cultivated areas, showcasing a tapestry of foliage with varying shades and textures. This dataset is crucial for ecological studies, land cover mapping, and environmental monitoring.

Natural Disaster Prone Area - Tsunami

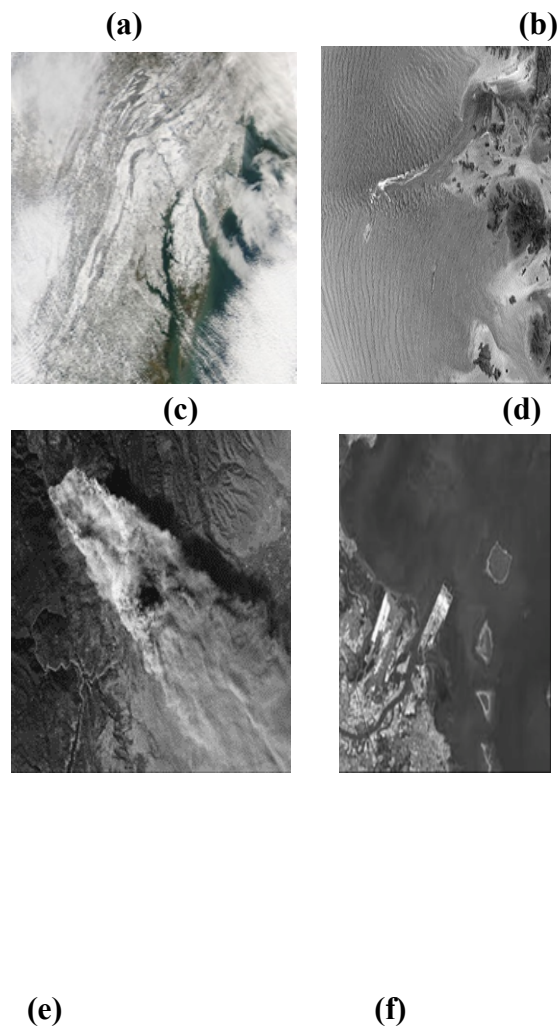
Fig. 6.f. documents the aftermath of a tsunami, capturing a landscape dramatically altered by the devastating force of the ocean's surge. The scene is marked by widespread destruction and disarray, with formerly populated areas now transformed into a chaotic mix of debris, mud, and remnants of structures. It captures the aftermath of a tsunami in a region that was once characterized by lush greenery. The devastating impact of the tsunami is evident as the vibrant green landscape has been dramatically altered. Large swaths of the green area are now submerged or covered in debris, indicating the forceful inundation of saltwater. The image may show signs of erosion along the coastlines, with the greenery replaced by muddy and barren terrain.

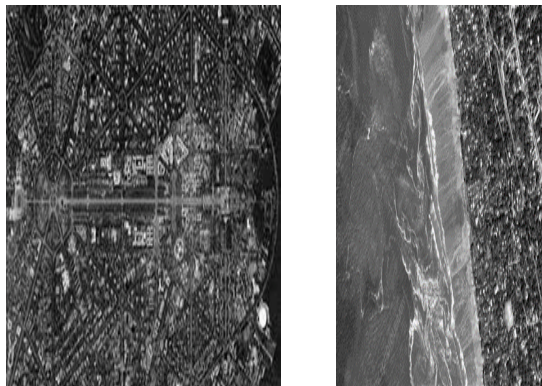
The image reveals the profound impact of a tsunami on a once-tranquil water area. The aftermath is characterized by a dramatically altered landscape, reflecting the devastating force of the tsunami's surges. Large bodies of water, such as coastal areas, rivers, or lakes, now exhibit signs of turbulence and upheaval. It is essential for assessing the impact of the tsunami on water

environments, understanding changes in coastal morphology, and guiding post-disaster recovery efforts.

Satellite Image Classification - Before and After Tsunami

Fig. 6.g. is part of a dataset designed for classifying areas impacted by a tsunami versus those that remain unaffected. The affected areas exhibit distinct characteristics indicative of the tsunami's destructive force. Along the coastlines, visible signs of inundation include changes in water color, sedimentation, and the displacement of debris. Conversely, unaffected regions maintain their natural features, displaying clear coastlines, undisturbed topography, and vibrant vegetation. Water bodies, whether rivers, lakes, or coastal regions, maintain their typical characteristics without the discernible signs of sedimentation or turbulence caused by the tsunami.





(g)

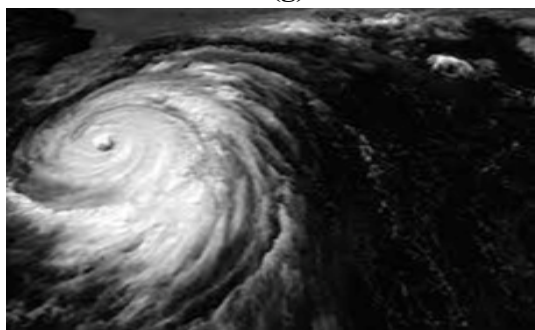


Fig. 6.Dataset **a.** Cloudy , **b.** desert , **c.** wildfire, **d.** water, **e.** green area , **f.** and **g.** Satellite images of Tsunami

d. water, **e.** green area , **f.** and **g.** Satellite

RESULTS

In this project, efforts were made to classify satellite images utilizing deep learning methodologies. Addressing a complex issue, different approaches have historically been employed. While successful outcomes have been achieved through feature engineering techniques, this project emphasized feature learning, a fundamental aspect of deep learning. We enhanced accuracy through rigorous training and testing processes.

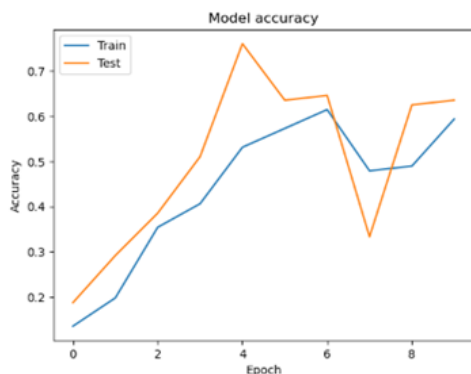


Fig. 7. Model accuracy with epoch

CONCLUSION

The application of artificial intelligence methods for classifying satellite images represents a significant breakthrough in remote sensing and data analysis. By exploring various machine learning and deep learning techniques, this effort has shown promise in transforming how we understand and apply satellite imagery. By tailoring and refining architectures that capture detailed spatial, spectral, and textural features within satellite images, we have achieved improved accuracy and efficiency in land cover classifications.

Future Work

Improving the network's accuracy and generalization can be achieved by implementing certain strategies. Firstly, leveraging the complete dataset during optimization can be advantageous. Batch optimization, especially suitable for larger datasets, can enhance performance. Moreover, individually evaluating satellite images can help identify those that pose greater classification challenges, facilitating targeted enhancement approaches.

REFERENCES

- [1] B. Al Homssi et al., “Next generation mega satellite networks for access equality: Opportunities, challenges, and performance,” *IEEE Commun. Mag.*, vol. 60, no. 4, pp. 18–24, Apr. 2022.
- [2] A Communications Alliance Satellite Services Working Group Paper, *Satell. Ind. Spectr. Strategy*, Commun. Alliance Ltd, North Sydney, NSW, Australia, 2022.
- [3] A. Gharanjik, B. Shankar M. R., P. Arapoglou, and B. Ottersten, “Multiple gateway transmit diversity in Q/V band feeder links,” *IEEE Trans. Commun.*, vol. 63, no. 3, pp. 916–926, Mar. 2015.
- [4] B. Xue, N. Tong, X. Xu, and X. He, “Dynamical short-term prediction of rain attenuation in W band: A time-series model with simpler structure and higher accuracy,” *IEEE Antennas Propag. Mag.*, vol. 61, no. 1, pp. 77–86, Feb. 2019.
- [5] A. D. Panagopoulos, P.-D.-M. Arapoglou, and P. G. Cottis, “Satellite communications at KU, KA, and V bands: Propagation impairments and mitigation techniques,” *IEEE Commun. Surveys Tuts.*, vol. 6, no. 3, pp. 2–14, 3rd Quart., 2004.
- [6] E. Cianca, T. Rossi, A. Yahalom, Y. Pinhasi, J. Farserotu, and C. Sacchi, “EHF for satellite communications: The new broadband frontier,” *Proc. IEEE*, vol. 99, no. 11, pp. 1858–1881, Nov. 2011.
- [7] B. A. Homssi et al., “Artificial intelligence techniques for next-generation mega satellite networks,” 2022, arXiv:2207.00414.
- [8] B. Al Homssi and A. Al-Hourani, “Optimal beamwidth and altitude for maximal uplink coverage in satellite networks,” *IEEE Wireless Commun. Lett.*, vol. 11, no. 4, pp. 771–775, Apr. 2022.
- [9] D. Roddy, *Satellite Communications*. New York, NY, USA: McGraw-Hill Education, 2006.

- [10] H. Xu, T. S. Rappaport, R. J. Boyle, and J. H. Schaffner, "Measurements and models for 38-GHz point-to-multipoint radio wave propagation," *IEEE J. Sel. Areas Commun.*, vol. 18, no. 3, pp. 310–321, Mar. 2000.
- [11] K. Simonyan and A. Zisserman, "Very deep convolutional networks for large-scale image recognition," in *Proc. Int. Conf. Learn. Representations*, pp. 106–120 (2015)
- [12] C. A. Laben and B. V. Brower, "Process for enhancing the spatial resolution of multispectral imagery using pan-sharpening", U.S. Patent 6,011,875, Jan. 4 (2000)
- [13] B. Aiazzi, S. Baronti, and M. Selva, "Improving component substitution pansharpening through multivariate regression of ms p pan data," *IEEE Trans. Geosci. Remote Sens.*, vol. 45, no. 10, pp. 3230–3239, Oct. (2007)
- [14] J. Choi, K. Yu, and Y. Kim, "A new adaptive component substitutionbased satellite image fusion by using partial replacement," *IEEE Trans. Geosci. Remote Sens.*, vol. 49, no. 1, pp. 295–309, Jan. (2011)
- [15] R. L. King and J. Wang, "A wavelet based algorithm for pan sharpening landsat 7 imagery," in *Proc. IEEE Int. Geosci. Remote Sens. Symp*, pp. 849–851 (2001)
- [16] B. Aiazzi, L. Alparone, S. Baronti, A. Garzelli, and M. Selva, "Multiscale fusion of high-resolution ms and pan imagery," *ISPRS J. Photogramm. Remote Sens.*, vol. 72, no. 5, pp. 591–596, (2006)
- [17] G. Masi, D. Cozzolino, L. Verdoliva, and G. Scarpa, "Pansharpening by convolutional neural networks," *Remote Sens.*, vol. 8, no. 7, Art. no. 594 (2016)
- [18] G. Scarpa, S. Vitale, and D. Cozzolino, "Target-adaptive CNNbased pansharpening," *IEEE Trans. Geosci. Remote Sens.*, vol. 56, no. 9, pp. 5443–5457, Sep. (2018)
- [19] J. Yang, X. Fu, Y. Hu, Y. Huang, X. Ding, and J. Paisley, "PanNet: A deep network architecture for pan-sharpening," in *Proc. IEEE Int. Conf. Comput. Vis*, pp. 5449–5457 (2017)
- [20] G. Scarpa, S. Vitale, and D. Cozzolino, "Target-adaptive CNNbased pansharpening," *IEEE Trans. Geosci. Remote Sens.*, vol. 56, no. 9, pp. 5443–5457, Sep (2018)
- [21] N. Akhtar, F. Shafait, and A. Mian, "Sparse spatio-spectral representation for hyperspectral image super-resolution," in *Proc. Eur. Conf. Comput. Vis.*, 2014, pp. 63–78.
- [22] Q. Wei, J. Bioucas-Dias, N. Dobigeon, and J.-Y. Tourneret, "Hyperspectral and

multispectral image fusion based on a sparse representation,” *IEEE Trans. Geosci. Remote Sens.*, vol. 53, no. 7, pp. 3658–3668, Jul. 2015.

[23] Q. Wei, N. Dobigeon, and J.-Y. Tourneret, “Bayesian fusion of multi band images,” *IEEE J. Sel. Top. Appl. Earth Observ. Remote Sens.*, vol. 9, no. 6, pp. 1117–1127, Sep. 2015.

[24] E. Wycoff, T. H. Chan, K. Jia, W. K. Ma, and Y. Ma, “A non-negative sparse promoting algorithm for high resolution hyperspectral imaging,” in *Proc. IEEE Int. Conf. Acoust. Speech Signal Process.*, 2013, pp. 1409–1413.

[25] C. Lanaras, E. Baltsavias, and K. Schindler, “Hyperspectral superresolution by coupled spectral unmixing,” in *Proc. IEEE Int. Conf. Comput. Vis.*, 2015, pp. 3586–3594.